

Contrast-Enhanced Magnetic Resonance Imaging at Earth's Magnetic Field Using Trace Gd^{3+} and Ho^{3+} Salts

Arthi S. Kozhumam¹, Lloyd Lumata², and Andhika Kiswandhi²

¹Westlake High School, Austin, TX

²University of Texas at Dallas, Richardson, TX

Summary

Here, we report a study of contrast-enhanced magnetic resonance imaging at Earth's field. In this study, we performed magnetic relaxation measurements of protons in water in the presence of the lanthanide ions Gd^{3+} and Ho^{3+} using the nuclear magnetic resonance technique. The results suggest that Gd^{3+} is a more effective T_1 and T_2 relaxation agent than Ho^{3+} and is therefore a better contrast agent. We then confirmed the relaxation phenomenon by performing a T_1 -weighted-contrast magnetic resonance imaging (MRI) of samples containing water doped with Gd^{3+} at the Earth's magnetic field. The T_1 -weighted imaging experimental result indicates that the intensity is the highest for the sample doped with the highest concentration of Gd^{3+} and lowest for the undoped sample. This work shows the feasibility of performing contrast-enhanced MRI in Earth's magnetic field using relaxation agents such as lanthanide ions. In addition, this work also demonstrates that, although the Earth's field MRI does not provide the strength and capability of a clinical MRI, it is still useful as a powerful demonstration tool, especially considering its low operating costs and portability.

Received: September 5, 2016; **Accepted:** February 9, 2017; **Published:** April 25, 2017

Copyright: (C) 2017 Kozhumam, Lumata, & Kiswandhi. All JEI articles are distributed under the attribution non-commercial, no derivative license (<http://creativecommons.org/licenses/by-nc-nd/3.0/>). This means that anyone is free to share, copy and distribute an unaltered article for non-commercial purposes provided the original author and source is credited.

Introduction

Magnetic resonance imaging (MRI) is a physics-based imaging technique that exploits the magnetic properties of nuclei to construct an image of the distribution of the nuclei (1). Because it probes only the magnetic properties, MRI has gained popularity as an imaging modality in the medical community to noninvasively obtain an anatomical image without using ionizing radiation or radioactive materials that may cause cell damage (2). As a magnetic resonance-based technique, MRI requires a homogeneous field. A homogeneous field with a strength of 1 Tesla (T) or more is commonly used for clinical purposes. Another

source of homogeneous field is the Earth's magnetic field, but its strength is typically no greater than 0.00005 T. Due to its weak strength, Earth's field MRI (EFMRI) is not commonly used and is mostly a novelty item for physics demonstrations. Moreover, the slow rate of data acquisition in EFMRI, which is associated with the low-strength field, makes contrast imaging challenging. In this work, we explore the possibilities of generating image contrast in EFMRI using an established procedure that is common in a clinical setting, namely by doping with trace paramagnetic salt.

MRI is based on NMR spectroscopy, developed specifically for spatial imaging. In NMR, nuclei are placed inside a magnetic field, where they precess around the magnetic field (B) in a manner similar to a tilted spinning top, as illustrated in **Figure 1a** (3). The precession frequency f , is proportional to the strength of the magnetic field according to the equation $f = \gamma B$, where γ and B are the nuclear gyromagnetic ratio and the magnitude of the magnetic field, respectively (1). The application of a radiofrequency (RF) pulse with the frequency f resonates with this precessional motion, effectively tipping the orientation of the nuclei to the xy plane (**Figure 1b**). Experimentally, the resonance can be achieved by placing the nuclei inside a coil that is located in an external field B as shown in **Figure 1c**. An RF pulse is then applied by an alternating current with the frequency f through the coil to tip the spin (usually by 90°), resulting in large magnetization in the xy plane. The precessional motion of the spins generates a time-varying magnetic flux inside the coil. Following Faraday's induction principle, the time-varying magnetic flux induces an alternating electrical current in the coil with a frequency f that can be measured. The spins will eventually reorient themselves towards the field due to the longitudinal (T_1) relaxation phenomenon while generating an oscillating current that decays with time due to transverse (T_2) relaxation, which is a signature of the NMR signal.

The main difference between NMR and MRI is the dimensionality. Whereas NMR is a one-dimensional spectroscopy technique, MRI can be one dimensional, two dimensional, or three dimensional. In MRI, an image is produced due to the magnetic-field gradient across the coil. Therefore, the magnetic field strength is different at every location within the coil. The implication

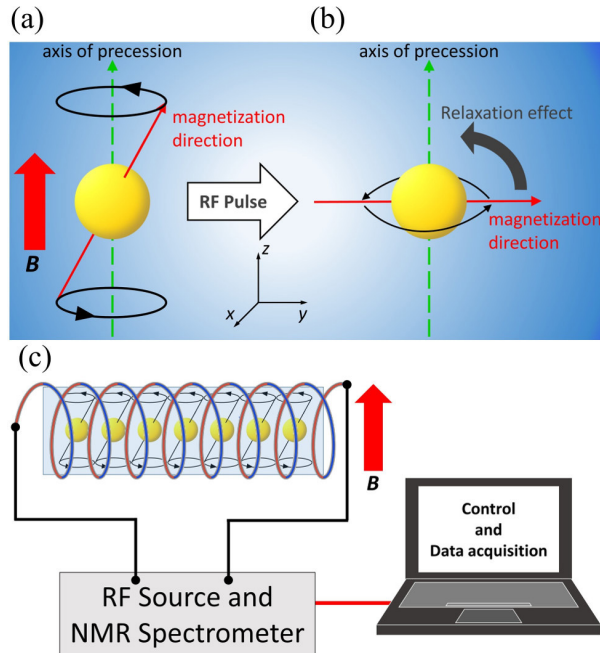


Figure 1: The behavior of a magnetic spin in the presence of an external magnetic field and the experimental setup to detect a magnetic resonance signal. (a) The precessional motion of a spin in a magnetic field B , whose frequency is known as the Larmor frequency. In the presence of the field, the magnetization of the spin is mostly directed parallel to the field. **(b)** An application of RF pulse tips the spin toward the xy plane, such that the largest magnetization is now located on the plane. **(c)** The experimental setup of an NMR experiment. The coil provides the RF pulse and acts as a detection coil when not pulsing. The coil is positioned such that the axis of the coil is perpendicular to the direction of the field B . The precessing nuclear spins can generate time-varying magnetic flux in the coil, which produces a current in the coil by the Faraday's induction law.

is that the nuclei at any coordinate within the coil (also known as an imaging bore in the case of MRI) will have a unique frequency. The function of an MRI spectrometer is to measure a collection of electrical signals of different frequencies and determine the locations within the imaging bore of the signals based on their frequencies. The presence of a signal at a certain frequency means nuclei (or an object) are present at a coordinate corresponding to that particular frequency. Similarly, the absence of a signal at a certain frequency is interpreted as the absence of the object at the coordinate defined by that frequency. Following this procedure, a spatial image can be reconstructed.

The use of superconducting electromagnets has been one of the requirements of MRI. This is partly due to the properties of a superconductor, which allow electrons to flow without resistance. Therefore, a superconducting coil is capable of sustaining an electrical current in a closed loop, thus maintaining a highly stable magnetic field for an extended period once energized without requiring an

external power source, making it an ideal electromagnet. The other requirement is a strong magnetic field, typically > 1 T, to reliably produce images with a high signal-to-noise ratio (SNR) (4). In recent years, however, there has been a growing interest in performing MRI at ultra-low magnetic field, such as Earth's magnetic field (5–11). Imaging with Earth's field takes advantage of its near-perfect homogeneity, which is globally available at no cost (8). This cost consideration is particularly crucial because superconductors have to be maintained at very cold temperatures, typically by using liquid helium, which is a non-renewable resource. In addition, EFMRI can potentially be set up in underdeveloped or rural areas, where helium might not be readily available. However, unlike the conventional MRI, EFMRI suffers from the lack of clarity and low resolution due to its low strength. Several methods have been used to improve the sensitivity of EFMRI, such as utilizing an integrated superconducting quantum interference device (SQUID) for signal detection (6, 7, 10) or hyperpolarized liquid (9, 11).

In imaging, aside from the SNR and the resolution, another important aspect in distinguishing two objects is the contrast between them. Contrast between two samples can be generated from the difference between the concentrations of nuclei present in the samples, in which the sample having a larger number of nuclei produces a brighter image. In addition, contrast can also be observed in samples having different nuclear relaxation times (1, 12). In clinical MRI, which probes the magnetism of hydrogen (^1H) nuclei, gadolinium ions in the form of Gd^{3+} (hereafter referred to as Gd for brevity) are widely used as a relaxation agent due to their effectiveness in reducing ^1H longitudinal relaxation time (T_1) via their paramagnetic relaxation effect (13–15). Therefore, the NMR signal of the Gd-doped ^1H has a different strength from the un-doped ^1H . Producing contrast in EFMRI, however, can be challenging due to the much lower SNR compared to the conventional MRI using a superconducting magnet (7). In order to improve the SNR, imaging is usually repeated several times and the signals averaged. In addition, to further improve the SNR, EFMRI typically involves a prepolarization/magnetization procedure to magnetize the nuclei before the MRI pulse sequence is applied. The prepolarization procedure is typically done using an additional strong electromagnet that encloses the MRI coil. The prepolarization step usually takes ~ 1 s. However, the averaging procedure in T_1 -weighted contrast MRI requires a quick repetition with < 1 s between two successive measurements (1, 12). Therefore, here we face the problem of how to simultaneously obtain an acceptable averaging and contrast. We expect that T_1 -contrast imaging in Earth's field is feasible if the

relaxation time of ^1H can be controlled by varying the concentration of Gd or changing Gd to another ion.

In addition to Gd, the paramagnetic relaxation effect can also be observed in other paramagnetic salts to a varying degree. Holmium ion in the form of Ho^{3+} (hereafter referred to as Ho for brevity) is an ion belonging to the lanthanide (Ln) family, but does not have the strength of Gd as a ^1H relaxation agent (14). The properties of both salts have been studied in strong magnetic fields, but their behavior in weak fields, such as the Earth's field, remains to be determined. Therefore, a study on the relaxation behavior of these lanthanides is desired as their behavior in strong fields may be different in weak fields.

In this article, we report our work on the magnetic relaxation times of ^1H using gadolinium or holmium as contrast agents. First, we studied the T_1 and T_2 of ^1H in water doped with GdCl_3 and HoCl_3 at various concentrations. Second, we studied the relaxation times of ^1H in the presence of Gd-DOTA and Ho-DOTA (DOTA = 1,4,7,10-tetraazacyclododecane-1,4,7,10-tetraacetic acid), which can be safely used in humans (16–19). Due to the toxicity of GdCl_3 and HoCl_3 and due to the limited amount of Gd-DOTA and Ho-DOTA available during this study, we limited our NMR studies to a field of 1 T, which allows smaller amounts of chloride and DOTA salts to be used. We note that this field is much larger than Earth's field, but we expect the results to provide some insights into the concentrations of Gd and Ho necessary for the EFMRI studies. Finally, we studied T_1 -weighted contrast MRI using GdCl_3 and HoCl_3 paramagnetic salts. We could not perform EFMRI using Gd-DOTA and Ho-DOTA, because large amounts of Gd-DOTA and Ho-DOTA are required for EFMRI. However, based on the information obtained from the relaxation time studies, we can predict how well they generate contrast compared to their chloride-salt counterparts. This work indicates that Gd remains a better contrast/paramagnetic relaxation agent at low fields compared to Ho and shows that

contrast can be generated using these paramagnetic salts by application of an appropriate set of MRI pulse parameters.

Results

The effects of lanthanide doping on ^1H relaxation times

We investigated the liquid-state relaxation properties of ^1H in weak fields in the presence of paramagnetic ions, such as Gd and Ho, assessing their ability to produce T_1 contrast in MRI in Earth's field. NMR measurement in Earth's field requires a large amount of sample, typically 500 ml of water, to compensate for the low SNR. Therefore, the relaxation measurements were performed using a commercial benchtop NMR spectrometer with an operating field of 1 T. This field is four orders of magnitude higher than Earth's field, but still considerably low compared to other commercially available spectrometers. The longitudinal relaxation time, T_1 , was measured using the inversion recovery method, in which spins are tipped to a direction opposite to the external field and return to the direction parallel to the field. The data were fitted to a monoexponential function

$$M_z(t) = M_0(1 - 2 \exp(-t/T_1)), \quad (1)$$

which describes a magnetization recovery characterized by a time constant T_1 and magnetization M_0 . The transverse magnetization decay is characterized by the time constant T_2 , following the equation

$$M_{xy}(t) = M_0 \exp(-t/T_2). \quad (2)$$

Figure 2a shows a ^1H NMR signal of water, which was used as a reference, taken at 1 T and 298 K. The signal (open squares) can be well fitted using a Lorentzian function (solid blue curve) as shown by the residual (solid green curve), which indicates that our benchtop NMR spectrometer could provide a sufficiently homogeneous field. The residual curve was shifted along the vertical axis for clarity. **Figures 2b and 2c** show the

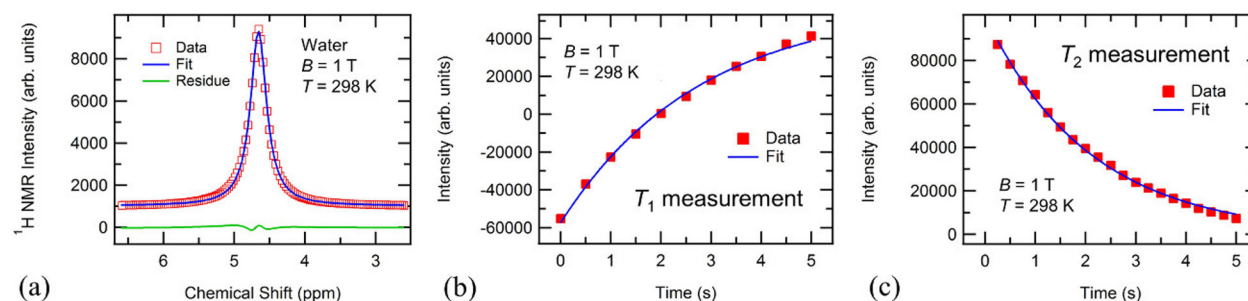


Figure 2: The representative NMR data and the analytical methods used to extract the relaxation times T_1 and T_2 . (a) ^1H (proton) NMR spectrum of water (reference) sample. The spectrum (square symbols) was fitted to a Lorentzian function (blue solid line). The data can be fitted satisfactorily as shown by the residue (green solid line). (b) The T_1 measurement of ^1H at $B = 1\text{ T}$. Shown here are the measurement result (squares) and the fitting result to equation 1 in the text. (c) The T_2 measurement of the same sample at $B = 1\text{ T}$ fitted to equation 2.

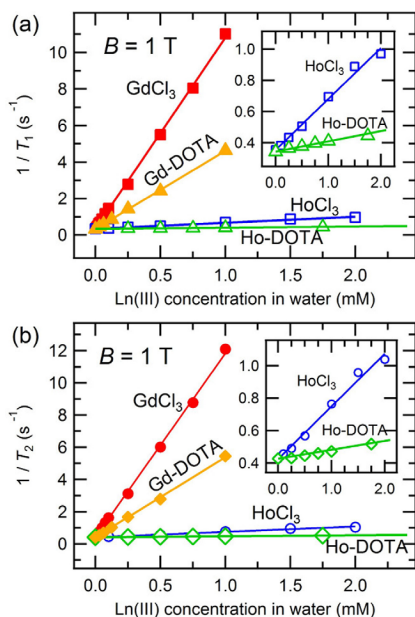


Figure 3: The effect of the concentration of Gd and Ho doping on the inverse of ^1H relaxation times measured at $B = 1\text{ T}$. (a) T_1^{-1} dependence on the concentration of GdCl_3 (red solid squares), Gd-DOTA (orange solid triangles), HoCl_3 (blue open squares), and Ho-DOTA (green open triangles). (b) T_2^{-1} dependence on the concentration of GdCl_3 (red solid circles), Gd-DOTA (orange solid diamonds), HoCl_3 (blue open circles), and Ho-DOTA (green open diamonds). The solid lines are the linear fit following equation 3. The insets show the inverse of relaxation times T_1 and T_2 of Ho-doped water, plotted separately for clarity, and the fitting result to equation 1 in the text. (c) The T_2 measurement of the same sample at $B = 1\text{ T}$ fitted to equation 2.

T_1 and T_2 fitting results, using equation 1 and 2, of ^1H in un-doped water. The analysis shows the T_1 and T_2 of ^1H in un-doped water as 2.82 s and 2.36 s, respectively.

Next, we obtained ^1H NMR relaxation data of water doped with various concentrations of chloride and DOTA salts of Gd and Ho, which are shown in **Figures 3a and 3b** plotted as the inverse of the relaxation times to show the correlation between the relaxation times and Ln concentrations. The plots show that both T_1^{-1} and T_2^{-1} of ^1H increase linearly with increasing concentrations of lanthanides. The data, accordingly, were fitted to the linear function (20, 21)

$$T_{1,2}^{-1}(C) = T_{1,2}^{-1}(0) + kC, \quad (3)$$

where C and k are the concentration of Ln and a proportionality constant that is dependent on the Ln species, respectively. Both T_1 and T_2 of un-doped reference water are known, so their values are fixed in the fitting. The values of k for all the contrast agents are listed in **Table 1**. Based on the k values, we see that GdCl_3 has the strongest relaxation effect on ^1H , followed by Gd-DOTA , HoCl_3 , and Ho-DOTA . Therefore, we expect that, given the same concentration, Gd-doped

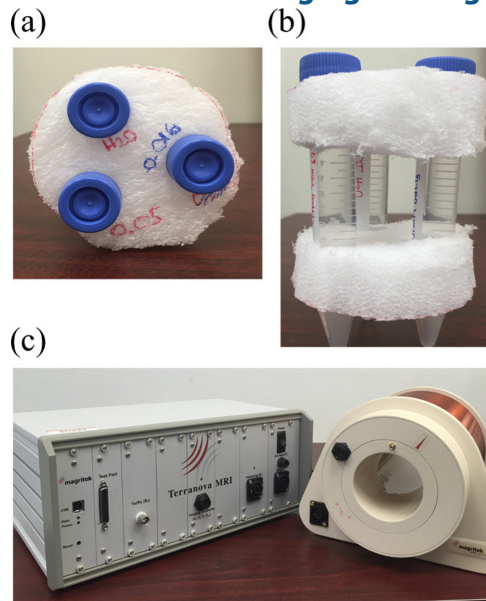


Figure 4: The phantom sample and the Terranova EFMRI system used. (a) The top view of the samples (phantom tubes). The phantom tubes consist of three 15-ml centrifuge tubes. (b) The side view of the phantom tubes. (c) The EFMRI system Terranova, shown here are the MRI coil and the spectrometer. In an actual experiment, the coil is positioned such that the axis of the solenoid is perpendicular to the North-South direction of the Earth's magnetic field.

sample will produce a larger contrast from the reference than the Ho-doped sample will.

Earth's field MRI

To demonstrate the feasibility of performing T_1 -weighted contrast MRI in Earth's field using Gd and Ho, we selected water samples doped with 0 mM (reference), 0.01 mM GdCl_3 , 0.05 mM GdCl_3 , 0.1 mM GdCl_3 , and 0.1 mM HoCl_3 . The samples were prepared as described in the Materials and Methods section and enclosed in 15-ml centrifuge tubes (**Figures 4a and 4b**). We used the commercial EFMRI system Terranova (Magritek, San Diego, CA; **Figure 4c**). The pulse sequence used for the study was designed to perform MRI with a fast repetition time, as required to produce T_1 -enhanced contrast

Contrast agent	k from T_1^{-1} fitting ($\text{s}^{-1}\text{mM}^{-1}$)	k from T_2^{-1} fitting ($\text{s}^{-1}\text{mM}^{-1}$)
GdCl_3	10.466 ± 0.071	11.418 ± 0.085
Gd-DOTA	4.280 ± 0.03	4.964 ± 0.05
HoCl_3	0.326 ± 0.009	0.325 ± 0.01
Ho-DOTA	0.07 ± 0.002	0.02 ± 0.003

Table 1: The k values obtained from the T_1^{-1} and T_2^{-1} data as a function of concentration of Gd^{3+} and Ho^{3+} by performing a linear fit to equation 3.

Parameter	Value
Matrix size	32 x 32
Field of view	100 mm x 100 mm
Polarizing duration	500 ms
B ₁ frequency	1543 Hz
Phase gradient duration	50 ms
Echo time	320 ms
Bandwidth	32 Hz
Repetition time	2 s

Table 2: The imaging parameters and their values used in this contrast-enhanced MRI study.

images. The pulse parameters are tabulated in **Table 2**.

First, we compared the resulting images from the reference, 0.1 mM GdCl₃ doping, and 0.1 mM HoCl₃ doping (**Figure 5a**). The result shows that Gd produces the brightest signal, while the reference sample gives a very weak signal. The Ho-doped sample produces a signal intensity between that of Gd-doped and undoped water. Both 1 T NMR and EFMRI show that Gd is a more effective relaxation/contrast agent compared with Ho. Because the relaxation times depend on the concentration, contrast can also be produced by varying the concentration of Ln ion in water. Comparison between the contrast produced by 0.01 mM and 0.05 mM GdCl₃ is displayed in **Figure 5b**. We observed that the sample with 0.05 mM GdCl₃ doping had the highest intensity.

Discussion

Due to its efficiency in reducing the T_1 and T_2 of ¹H in water, Gd has been used widely to enhance contrast in MRI (13, 14, 16). The efficiency of Gd as a contrast/relaxation agent is demonstrated by the large changes in the T_1 and T_2 of ¹H upon changing the Gd concentration, which is characterized by k in equation 3. Our results show that in weak fields Gd remains a more effective relaxation/contrast agent than Ho. Image contrast can be designed to be dependent mostly on T_1 or T_2 by using appropriate imaging parameters. T_1 -weighted contrast enhancement requires imaging with a fast repeat time to produce contrast between two regions having different relaxation times.

Fast repetition can be difficult to achieve in EFMRI due to the prepolarization procedure before the RF pulse. The polarizing duration is typically on the order of ~1 s, and up to 4 s can be used with the Terranova EFMRI during normal operation, limiting the repetition rate. In practice, the coil duty cycle has to be considered as well. Duty cycle is a measure of how long the prepolarization coil is energized during one signal acquisition. This duty cycle has to be minimized to avoid overheating the coil by either reducing the polarization time or extending the repeat time. Because a short repeat time is required

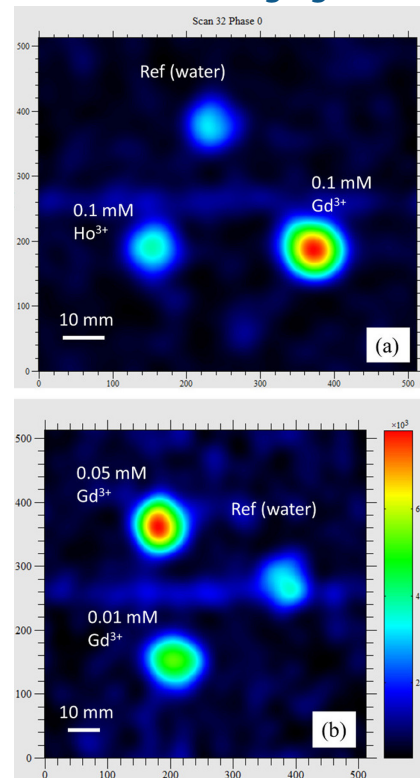


Figure 5: Imaging experiment in Earth's field on the phantom tubes containing various concentrations of GdCl₃ and HoCl₃. (a) The comparison of the results of the T_1 contrast-enhanced MRI in Earth's magnetic field using 0.1 mM GdCl₃ and 0.1 mM HoCl₃. (b) The result of T_1 -contrast enhanced MRI using 0.05 mM GdCl₃ and 0.01 mM GdCl₃. The images have been extrapolated from 32 × 32 matrix size to 512 × 512.

to perform T_1 -weighted contrast MRI, we reduced the polarization time at the expense of lower SNR.

We were able to obtain T_1 -enhanced contrast in Terranova EFMRI by using trace GdCl₃ and HoCl₃ with a concentration of 0.1 mM. The T_1 of ¹H is 2.8 s, 2.6 s, and 0.7 s for the reference (water), 0.1 mM Ho, and 0.1 mM Gd, respectively (**Figure 3a**). We can explain the resulting contrast by considering the signal intensity formula as a function of T_1 and T_2 , ¹H density (N), repetition time (TR), and the echo time or the acquisition delay time (TE) given by (1)

$$I(T_1, T_2, TR, TE) = N(1 - e^{-TR/T_1})e^{-TE/T_2}. \quad (4)$$

First, the factor N is determined by the number of ¹H nuclei in the sample, so the more nuclei present in the sample, the larger the intensity is. Second, equation 4 implies that a shorter T_1 increases the intensity and a shorter repeat time increases the T_1 weighting. Third, we have to consider the T_2 effect in the last factor. A shorter T_2 reduces the intensity, but its contribution to the intensity can be minimized by using a short TE , such that the ratio TE/T_2 is small, meaning that the acquisition has to be taken as soon as possible after the application of

the 90° pulse. Both Gd and Ho reduce T_1 and T_2 , so there is a competing effect between the intensity gain and loss due to the reduced T_1 and T_2 , respectively.

For imaging, we chose a polarization time of 500 ms, which is lower than the usual 4 s, while maintaining a 25% duty cycle, resulting in a repeat time (TR) of 2 s. In the Terranova EFMRI, a polarization time of 500 ms corresponds to the lowest recommended value for this parameter. Our chosen TR value is relatively long, considering T_1 is reduced by Ln doping to about 680 ms with 0.1 mM $GdCl_3$. In order to increase the T_1 contribution, we minimized the T_2 contribution by selecting an echo time (TE) of 320 ms. Using these parameters in equation 4 and assuming that the T_1 and T_2 results obtained at $B = 1$ T remain valid at Earth's field, we can analyze our result as the following. First, because the volume of water is the same for every tube, we can neglect the factor N , which depends only on the 1H density in the samples. Second, neglecting the T_2 factor, our choice of $TR = 2$ s gives intensities 86% and 5% higher than water for the 0.1 mM $GdCl_3$ -doped and the 0.1 mM $HoCl_3$ -doped samples, respectively. Third, the contribution from T_2 relaxation reduces the intensity by 13%, 41%, and 14% for the un-doped, 0.1 mM $GdCl_3$ -doped, and 0.1 mM $HoCl_3$ -doped water, respectively. Combining all the factors, we can calculate the relative intensity enhancements, which are 27% for the 0.1 mM $GdCl_3$ -doped sample and 4% for the 0.1 mM $HoCl_3$ -doped sample. The intensities of the un-doped water and the 0.1 mM Ho -doped sample are similar, while the 0.1 mM Gd -doped sample gives the highest intensity (**Figure 5a**). Following the same procedures, we obtained 17% relative enhancement for the 0.01 mM $GdCl_3$ -doped sample and 35% for the 0.05 mM $GdCl_3$ -doped samples. **Figure 5b** shows that the 0.01 mM $GdCl_3$ -doped sample had an intensity between the un-doped and 0.05 mM $GdCl_3$ -doped water. However, by examining the color scale, it is apparent that, while our calculation can qualitatively explain the achieved contrast, it does not agree quantitatively with the experimental data. According to our data, the 0.1 mM $GdCl_3$ -doped sample had a relative intensity more than 100% higher than the un-doped water or the $HoCl_3$ -doped sample. In addition, the relative intensity of the 0.01 mM $GdCl_3$ -doped sample was about 50% higher or more than that of the un-doped water. The difference between the experimentally obtained and the calculated relative intensities may be attributed to the effect of the prepolarization procedure and the fact that the relaxation measurements were performed at $B = 1$ T, which may not correctly reflect the values of relaxation times in Earth's field. We assert that the prepolarization procedure contributes significantly to the intensity because it polarizes the sample before the application of the 90° pulse. A sample with a lower T_1 can be

polarized faster, which gives a higher magnetization and consequently a higher signal. Therefore, there might be an additional factor in equation 4 that has to be included when a prepolarization procedure is used, which is likely dependent upon T_1 , polarizing time, and the magnitude of the polarizing field.

We have to point out that our EFMRI studies were performed using unchelated Ln compounds. Unchelated Gd is physiologically toxic, thus requiring chelation ligands to prevent it from being released into the body (13, 16, 17). Therefore, we performed relaxation studies of chelated Ln, in particular using DOTA ligand as a chelator, which is known to be highly stable in physiological conditions (18, 19). Although we could not perform EFMRI studies using Gd-DOTA and Ho-DOTA, we may predict how well they produce contrast based on the relaxation data from our 1 T NMR studies. By comparing the contrast produced by $GdCl_3$ and $HoCl_3$, we observed that T_1 contrast is better with a contrast agent that gives a shorter T_1 . That is, T_1 contrast is produced between two substances when the difference between the T_1 of the two is large. The T_1 of 1H in the presence of Gd-DOTA was between the reference and the $GdCl_3$ -doped water. Therefore, we expect that given the same pulse sequence and doping concentration, the contrast between the Gd-DOTA-doped sample and the reference will be weaker than it would be between the $GdCl_3$ -doped sample and reference. In addition, the Ho-DOTA-doped sample will produce very little contrast compared with the reference sample.

In conclusion, we have shown that the addition of Gd and Ho into the samples can reduce the relaxation times T_1 and T_2 of 1H . Gd is a more efficient MRI relaxation agent compared to Ho. T_1 -weighted contrast MRI can be obtained in Earth's magnetic field using a Terranova system EFMRI. Using a proper set of parameters involving a short repetition time and a short echo time, stark contrast between the three phantom samples can be produced, where the sample with the lowest T_1 produced the strongest signal while the pure water sample produced the weakest signal due to its long T_1 .

Methods

$GdCl_3$ and $HoCl_3$ were obtained commercially (Sigma-Aldrich, St. Louis, MO) as $GdCl_3$ hexahydrate and $HoCl_3$ hexahydrate and used without further purification. The DOTA salts were synthesized following the procedure given in ref. (19). The samples were prepared by diluting the ions to the required concentrations.

The relaxation times of protons in the samples doped with various concentrations of Gd and Ho were measured using the 1 T benchtop NMR system Spinsolve (Magritek, San Diego, CA) and compared to a reference sample of pure water. The NMR spectra were

analyzed by the programs SpinWorks 4 and Mestrenova (Escondido, CA). The relaxation times T_1 and T_2 were quantified by using monoexponential fittings given by equation 1 and equation 2, respectively.

The MRI studies were carried out using the EFMRI system Terranova (Magritek, San Diego, CA) on the samples doped with $GdCl_3$ and $HoCl_3$. Samples containing 0.1 mM $GdCl_3$ and 0.1 mM $HoCl_3$ were selected to compare the effects of Gd and Ho doping in contrast-enhanced MRI. To compare the effect of Gd concentration in producing contrast, samples containing 0.01 mM and 0.05 mM $GdCl_3$ were chosen based on their T_1 and T_2 values.

Prior to performing the imaging experiments, the MRI system was positioned away from any magnetic materials, including the walls of the laboratory. A compass was used to align the axis of the coil perpendicular to the North-South direction (x -axis). A three-dimensional compass was then used to find the direction of the Earth's magnetic flux in order to define the second axis (z -axis). After the coil had been properly positioned and oriented, the 1H signal was measured using 1D NMR on a bottle containing 500 ml of water. The system was then shimmed using an automatic procedure provided in the software package to homogenize the field inside the MRI system.

The samples for the MRI studies were contained in phantom tubes made using three 15-mL centrifuge tubes secured with a piece of styrofoam (**Figures 3a and 3b**). The tubes were placed 40 mm apart. The position of the tubes in the coil and the corresponding position in the image were verified by removing and replacing the tubes and performing MRI. Each tube contained a sample with a different type of lanthanide: 0.01 mM $GdCl_3$, 0.05 mM $GdCl_3$, 0.1 mM $GdCl_3$, 0.1 mM $HoCl_3$, or 0 mM (water as a reference). The 2D MRI was performed by averaging over 32 scans in order to enhance the signal-to-noise ratio. The parameters were chosen to minimize the repetition time while maintaining the coil duty cycle at less than 25% to avoid overheating the polarizing coil. The imaging parameters and their values are shown in **Table 2**. The resulting images were extrapolated from 32×32 matrix size to 512×512 matrix size by using an extrapolation procedure provided in the software package.

Acknowledgements

The authors would like to acknowledge the support from the Robert A. Welch Foundation grant no. AT-1877. The Welch summer scholar program at the University of Texas at Dallas is sponsored by the Robert A. Welch Foundation

References

1. Hashemi, Ray H., William G. Bradley, and Christopher J. Lisanti. *MRI : The Basics*. Philadelphia: Lippincott Williams & Wilkins, 2010. Print.
2. "Magnetic Resonance Imaging (MRI)." *National Institute of Biomedical Imaging and Bioengineering*. N.p., 13 May 2013. Web. 28 Aug. 2016.
3. Hore, Peter J. *Nuclear Magnetic Resonance*. Oxford: Oxford University Press, 2015. Print.
4. Aarnink, René, and Johan Overweg. "Magnetic Resonance Imaging, a Success Story for Superconductivity." *Europhysics News* 43.4 (2012): 26–29. Print.
5. Mohorič, Aleš et al. "Magnetic Resonance Imaging System Based on Earth's Magnetic Field." *Instrumentation Science & Technology* 32.6 (2004): 655–667. Print.
6. McDermott, Robert et al. "Microtesla MRI with a Superconducting Quantum Interference Device." *Proceedings of the National Academy of Sciences of the United States of America* 101.21 (2004): 7857–7861. Print.
7. Lee, Seung Kyun et al. "SQUID-Detected MRI at 132 μT with T_1 -Weighted Contrast Established at 10 μT –300 mT." *Magnetic Resonance in Medicine* 53.1 (2005): 9–14. Print.
8. Halse, Meghan E. et al. "A Practical and Flexible Implementation of 3D MRI in the Earth's Magnetic Field." *Journal of Magnetic Resonance* 182.1 (2006): 75–83. Print.
9. Halse, Meghan E., and Paul T. Callaghan. "A Dynamic Nuclear Polarization Strategy for Multi-Dimensional Earth's Field NMR Spectroscopy." *Journal of Magnetic Resonance* 195.2 (2008): 162–168. Print.
10. Inglis, Ben et al. "MRI of the Human Brain at 130 Microtesla." *Proceedings of the National Academy of Sciences* 110.48 (2013): 19194–19201. Print.
11. Coffey, Aaron M. et al. "High-Resolution Low-Field Molecular Magnetic Resonance Imaging of Hyperpolarized Liquids." *Analytical Chemistry* 86.18 (2014): 9042–9049. Print.
12. Westbrook, Catherine., Carolyn Kaut. Roth, and John Talbot. *MRI in Practice*. Chichester, West Sussex; Malden, MA: Wiley-Blackwell, 2011. Print.
13. Caravan, Peter et al. "Gadolinium(III) Chelates as MRI Contrast Agents: Structure, Dynamics, and Applications." *Chemical Reviews* 99.9 (1999): 2293–2352. Print.
14. Norek, Małgorzata, and Joop A. Peters. "MRI Contrast Agents Based on Dysprosium or Holmium." *Progress in Nuclear Magnetic Resonance Spectroscopy* 59.1 (2011): 64–82. Print.
15. Bakhmutov, Vladimir I. *Practical NMR Relaxation for Chemists*. Chichester, West Sussex, England: Wiley,

2004. Print.
- 16.Hermann, Petr et al. "Gadolinium(III) Complexes as MRI Contrast Agents: Ligand Design and Properties of the Complexes." *Dalton Transactions* 23 (2008): 3027–3047. Print.
 - 17.De Broe, Marc E. "Can the Risk of Gadolinium Be Extrapolated to Lanthanum?" *Seminars in Dialysis* 21.2 (2008): 142–144. Print.
 - 18.Babailov, Sergey P., Peter V. Dubovskii, and Eugeny N. Zapolotsky. "Paramagnetic Lanthanides as Magnetic Resonance Thermo-Sensors and Probes of Molecular Dynamics: Holmium-DOTA Complex." *Polyhedron* 79 (2014): 277–283. Print.
 - 19.Martins, André F. et al. "A Bis(pyridine N-Oxide) Analogue of DOTA: Relaxometric Properties of the GdIII Complex and Efficient Sensitization of Visible and NIR-Emitting Lanthanide(III) Cations Including PrIII and HoIII." *Chemistry – A European Journal* 20.45 (2014): 14834–14845. Print.
 - 20.Kang, Young S., John C. Gore, and Ian M. Armitage. "Studies of factors affecting the design of NMR contrast agents: manganese in blood as a model system." *Magnetic Resonance in Medicine* 1.3 (1984): 396-409. Print.
 - 21.Yilmaz, A., M. Yurdakoç, and B. Işık. "Influence of transition metal ions on NMR proton T_1 relaxation times of serum, blood, and red cells." *Biological Trace Element Research* 67.2 (1999): 187-193. Print.